

Modeling acute ethanol-induced impairment with gastric organoids

Wanjuan Wang

Beijing University of Chinese Medicine

Ying Zhao

Beijing University of Chinese Medicine Third Affiliated Hospital

Zeqi Su

Beijing University of Chinese Medicine

Fuhao Chu

Beijing University of Chinese Medicine

Tao Li

Beijing University of Chinese Medicine

Yuan Li

Beijing University of Chinese Medicine

Xiaoyu Song

University of Science and Technology of China

Xu Liu

University of Science and Technology of China

Xing Liu

China University of Science and Technology

Xia Ding (✉ dingx@bucm.edu.cn)

<https://orcid.org/0000-0002-7346-942X>

Research article

Keywords: Stomach organoids, Ezrin, Murine, Alcohol

Posted Date: January 14th, 2021

DOI: <https://doi.org/10.21203/rs.3.rs-42294/v2>

License: © ⓘ This work is licensed under a Creative Commons Attribution 4.0 International License.

[Read Full License](#)

Abstract

Background: Ethanol has been linked to atrophic gastritis and gastric carcinoma. Although it is well known that ethanol can result in hypochlorhydria, the molecular mechanisms underlying this phenomenon remain poorly understood.

Results: Here we used gastric organoids to show that ethanol permeabilized the apical membrane of gastric parietal cells and induced ezrin hypochlorhydria. The functional consequences of ethanol on parietal cell physiology were studied using organoids. Gastric organoids were pre-incubated in the basic medium or with EGTA or E64, and incubated at 37°C in either medium alone, or medium containing 6% ethanol. We assessed ezrin proteolysis. Ethanol permeabilization induced activation of calpain and subsequent proteolysis of ezrin, which resulted in the liberation of ezrin from the apical membrane of the parietal cells. Significantly, expression of calpain-resistant ezrin restored the functional activity of parietal cells in the presence of ethanol.

Conclusion: Taken together, our data indicated that ethanol disrupted the apical membrane-cytoskeleton interactions in gastric parietal cells and thereby caused hypochlorhydria.

Background

The stomach tends to be exposed to various toxic factors, and ethanol is the most common factor that might contribute to the pathogenesis of various gastrointestinal (GI) dysfunctions, including gastritis, gastric ulcer, or even gastric carcinoma¹. Currently, the majority of knowledge about the cellular and molecular mechanisms of toxicity caused by ethanol relies on experiments performed in animal models or cell models. However, the stomachs of different species vary widely in their morphology, the intricacy of their stomach networks and their topographical organizations. Therefore, it is difficult to gain a precise understanding of the effects of acute alcoholic-induced parietal injury in humans.

Human adult stomach stem cells have been recently reported to enable the self-organization of millimeter-size, complex 3D stomach tissues with unprecedented morphogenetic and histological realism *in vitro*, referred to as gastric organoids^{2,3}. This near-physiological and self-renewing 3D organoid sustain similar organ functionality as the stomach. To date, gastric organoids have been used to establish various models of gastric diseases including *Helicobacter pylori* infection⁴ and proved to be powerful as a 3D platform for the investigation of psychiatric disease origin and pathology *in vitro*.

Gastric acid secretion and the process of regulation by the cAMP-dependent protein kinase, protein kinase A (PKA) pathway are involved in phosphorylation of the cytoskeletal protein ezrin, which was an 80-kDa microvilli-rich micro vessel. Ezrin protein belongs to the family of widely distributed cell membrane-associated proteins, the ezrin/radixin/moesin protein family⁵, whose initial isolation is based on the dependence of ezrin on the phosphorylation of PKA in stimulated parietal cells^{6,7}. Ezrin protein is mainly expressed in epithelial cells and distributed prior to the protrusion part of the cell surface: such as

microvilli rich in actin, folds of cell membranes, filamentary pseudopodia rich in skeletal protein, stretched cell front, and various local adhesions and so on. Ezrin is polarized in the apical canalicular membrane of gastric parietal cells and is an essential component of gastric acid secretion⁸. When ezrin proteins were knocked out in mice, the vesicles of the proton pump to the apical membrane were unable to form and the normal functions were lost⁹, leading to severe defects in gastric acid secretion and death within three weeks¹⁰.

Herein, we presented a stem cell-based gastric organoid model that allows the exploration of acute ethanol-induced pathogenesis of gastric development *in vitro* (Fig. 1). When exposed to ethanol, gastric organoids were impaired in comparison with the controls, including the diameter and morphology, and proteolysis of ezrin.

Results

Establishment of murine gastric organoids. To observe the protein markers in the growth process of gastric organoids, H⁺, K⁺ - ATPase (marker of parietal cells), ezrin (marker of apical membrane), F-actin and DAPI were detected by immunofluorescence on day 1, 3, 5 and 7 respectively, and images were taken with confocal microscope (Fig. 1). Murine gastric organoids expressed ezrin protein, which is in accordance with the stomach *in vivo* and indicated that the apical membrane of murine gastric organoids was oriented towards the lumen and had polar distribution. The presence of H⁺, K⁺ - ATPase suggested that the model system could be used to study the physiological and pathological characteristics of parietal cells.

In order to further semi quantitatively observe the changes of protein markers in the growth process of stomach organoids, murine gastric organoids were collected on the 1st, 3rd, 5th, 7th, 9th and 11th day respectively, and the distribution of H⁺, K⁺ - ATPase, ezrin and F-actin were detected by western blot. The results showed that the protein markers of murine gastric organoids remained stable in Day 5-9 (Fig. 1, d).

Ethanol impaired gastric organoids. In order to observe the effect of different concentrations of ethanol on gastric organoids, EtOH were added to the medium with organoids and the final concentrations were 0%, 2%, 4%, 6%, and 8%. One hour later, the organoids were stained by 0.4% trypan blue solution to detect cell death and images were taken under inverted fluorescence microscope (Olympus X81). Statistical analysis of organoids with positive trypan blue staining was carried out. As shown in Figure 2, the final concentration of EtOH leading to LD50 (Lethal Dose 50) was 6%. However, when the concentration of EtOH exceeded 10%, the Matrigel tended to dissolve and collapse.

In order to dynamically observe the impairment of 6% ethanol on the gastric organoids, the living gastric organoids were stained with Hoechst for 30 minutes, and then were placed under the microscope. The final concentration of ethanol was 6% and the images were taken. The imaging time was 30 minutes. 30 minutes later, the nuclei of murine gastric organoids shrunk and the lumen became narrower (Fig. 2, b).

Considering that the center of the gastric tube was a cystic luminal structure, and due to the concentration limitation of ethanol added to the medium, microinjection was used to inject the ethanol into the lumen of the gastric organoids (Fig. 2, c). One hour later, the samples were subjected to western blotting or immunofluorescence staining to observe impairment on gastric organoids. However, one hour after 6% ethanol was injected into the gastric organoids, no obvious impairment was observed. Next, we increased the concentration of ethanol to 50%. After 1 hour, we observed the death of organoids. As shown in Fig. 2, c, the gastric organoids were cultured, and microinjections of ethanol at different concentrations were performed on Day 6 of the organoids. One hour after microinjection of 50% ethanol into the organoids, the apical membrane marker ezrin and the parietal cell marker H^+ , K^+ -ATPase were destroyed, and the lumens of the organoids collapsed.

Next, the murine gastric organoids were impaired with EtOH added to the medium at a final concentration of 6%, and western blotting was performed at 0, 15, 30, 45, and 60 minutes. It was found that there was a cleaved ezrin in 55kDa and the band had a tendency of becoming more and more obvious over time (Fig. 2, d).

Immunofluorescence staining of ezrin, F-actin and DAPI (Fig. 3, a), or H^+ - K^+ -ATPase, ezrin and DAPI (Fig. 3, b) was performed 1 hour after gastric organoids were impaired by 6% ethanol added to the medium with a time gradient of 0-90 minutes. As can be seen from Fig. 3, a, with the prolongation of time, the location of ezrin gradually became diffused, and the lumen of organoids shrunk.

Ethanol-induced organoids impairment was caused by calcium-dependent calpain activation. To investigate whether the impairment of ethanol-mediated gastric organoids was caused by calcium-dependent calpain activation, gastric organoids were divided into four groups: 1.8 mM $CaCl_2$ group, 1.8 mM $CaCl_2$ plus 6% ethanol group, 1.8 mM $CaCl_2$ plus 6% ethanol plus 100 μ M E64 (calpain inhibitor) group and 30 μ M BAPTA (extracellular calcium chelator) plus 1.8 mM $CaCl_2$ plus 6% ethanol group. The murine gastric organoids were injured for 1 hour, and then samples were taken to run western blot to detect calpain I, ezrin and F-actin. Image J was used to measure the gray value of the strips. As a result, the hydrolyzed band of ezrin in the 1.8 mM $CaCl_2$ plus 6% ethanol group increased, and the difference was statistically significant ($p < 0.001$) (Fig. 3, d).

To investigate whether alcohol-mediated gastric organoid damage is caused by calcium ions, we divided murine gastric organoids into four groups: 1.8 mM $CaCl_2$ group, 1.8 mM $CaCl_2$ plus 6% EtOH group, 1.8 mM $CaCl_2$ plus 6% EtOH plus 2 mM EGTA (intracellular calcium chelator) group and 30 μ M BAPTA (extracellular calcium chelator) plus 1.8 mM $CaCl_2$ plus 6% EtOH group. Murine gastric organoids were impaired for 1 hour, and then samples were taken for western blot analysis and H^+ , K^+ -ATPase, Ezrin and F-actin were detected. Image J was used to measure the gray value of the strips. Compared with the 1.8 mM $CaCl_2$ plus 6% EtOH group, the hydrolysis bands of Ezrin in BAPTA plus 1.8 mM $CaCl_2$ plus 6% ethanol group and 1.8 mM $CaCl_2$ plus 6% EtOH plus 2 mM EGTA group were significantly decreased, and the difference was statistically significant ($p < 0.001$) (Fig. 3, d).

Ethanol-mediated calcium ion impairment on the localization of ezrin, H⁺, K⁺-ATPase and F-actin in murine gastric organoids. To investigate the effects of ethanol-mediated calcium impairment on the localization of ezrin and F-actin in murine gastric organoids, we divided murine gastric organoids into five groups: 1.8 mM CaCl₂ group, 1.8 mM CaCl₂ plus 6% EtOH group, 1.8 mM CaCl₂ plus 6% EtOH plus 2 mM EGTA (intracellular calcium chelator) group, 30 μM BAPTA (extracellular calcium chelator) plus 1.8 mM CaCl₂ plus 6% EtOH group and 1.8 mM CaCl₂ plus 6% EtOH plus 100 μM E64 (calpain inhibitor) group. The murine gastric organoids were impaired for 1 hour, followed by sample fixations, and the expressions of H⁺, K⁺-ATPase, ezrin and F-actin were detected by in situ immunofluorescence, and photographed by confocal microscopy LSM880.

Over time, the localization of ezrin in the apical membrane of organoids in the 1.8mM Ca²⁺ plus 6% EtOH group were dispersed, while the ezrin in the groups of 1.8mM Ca²⁺+6% EtOH plus EGTA (intracellular calcium chelator) group, 1.8mM Ca²⁺ plus 6% EtOH plus BAPTA (extracellular calcium chelator) group and the 1.8 mM Ca²⁺ plus 6% EtOH plus E64 (calpain inhibitor) group localized in the apical site was clear (Fig. 4).

To investigate the effects of ethanol-mediated calcium damage on the localization of ezrin and H⁺, K⁺-ATPase in murine gastric organoids, murine gastric organoids were divided into five groups: 1.8 mM CaCl₂ group, 1.8 mM CaCl₂ plus 6% EtOH group, 1.8 mM CaCl₂ plus 6% EtOH plus 2 mM EGTA (intracellular calcium chelator) group, 30 μM BAPTA (extracellular calcium chelator) plus 1.8 mM CaCl₂ plus 6% EtOH group and 1.8 mM CaCl₂ plus 6% EtOH plus 100 μM E64 (calpain inhibitor) group. One hour later, the impaired murine gastric organoids were fixed and the expressions of H⁺, K⁺-ATPase and ezrin were detected by in situ immunofluorescence and photographed by confocal microscopy LSM880.

Over time, the localization of ezrin in the apical membrane of 1.8mM Ca²⁺ plus 6% EtOH group became blurred and diffused, while the localization of ezrin remained clear in the 1.8mM Ca²⁺ plus 6% EtOH plus EGTA (intracellular calcium chelator) group, 1.8mM Ca²⁺ plus 6% EtOH plus BAPTA (extracellular calcium chelator) group and the 1.8 mM Ca²⁺ plus 6% EtOH plus E64 (calpain inhibitor) group, and the localization of H⁺, K⁺-ATPase did not change significantly (Fig. 4,b).

To investigate the effect of ethanol-mediated calcium ion on ezrin expression in human gastric organoids, human gastric organoids were injured either with 1.8 mM CaCl₂, 1.8 mM CaCl₂ plus 6% EtOH, or with 1.8 mM CaCl₂ plus 6% EtOH plus E64 (calpain inhibitor), respectively. After 1 hour, samples were collected for western blot, and the expressions of ezrin and actin were detected, and the values of the bands were measured with Image J (Fig. 5).

As can be seen from Fig. 5, ezrin in the 1.8 mM CaCl₂ + 6% EtOH group showed significant hydrolysis, suggesting an increase in the activity of calpain I. In the E64d group, no significant hydrolysis of ezrin was

observed. There was no significant increase in calpain I activity, and the difference was statistically significant in the E64 group compared with the alcohol group ($p < 0.05$).

Discussion

Before the origin of organoid system, most of the studies of gastric diseases were modeled using cell lines, animal models or explants, and these model systems have their own limitations¹¹.

The gastric epithelial cell line is a commonly used model system for studying gastric diseases, which was originally derived from gastric tumors. Their advantages are immortalized, readily available, easy to culture and can be applied to a variety of experiments. However, its molecular characteristics have been modified, including tumor suppressor genes, oncogenes, and cell cycle regulatory genes, and thus there is a certain gap with epithelial cells in physiology. Cell lines accumulate mutations during in vitro culture for decades, and some cell lines are infected with viruses, such as AGS cell lines, which are usually infected with type β parainfluenza virus, affecting pathways involved in immunity, proliferation and tumorigenesis, and interferon responses¹².

Conventional tumor cell culture is two-dimensional, but studies have shown that whether cell lines grew in 2D or 3D can affect drug efficiency¹³. This suggests that 3D is an important feature of tissue response. However, 3D cell spheres cultured from a single cell line lack a combination of different cell types typical of tissues and organs, while gastric organoids may include parietal cells, chief cells, cervical mucus cells, stem cells, and endocrine cells, etc.

Primary cell culture models are often a good alternative to tumor cell lines because they have not been transformed. Primary cultured gastric parietal cells have polarized structural features and polarized exocytosis and endocytosis, and were easy to access to large amounts. However, these cells are unable to self-renew and cannot be cultured and expanded for a long time, and all of the original cells need to be freshly isolated for each experiment.

The animal model system is more holistic and dynamic than the cell line, but some human stomach diseases cannot be responded to by animal models. For example, after mice were infected with *Helicobacter pylori*, they often only have mild gastritis and would not progress to gastric ulcer or stomach cancer. Mongolian gerbils can progress to gastric cancer after infection with *Helicobacter pylori*, but its distant line limits its researches and applications¹⁴.

The gastric organoids include parietal cells, chief cells, cervical mucus cells, stem cells, and endocrine cells which are also contained in the fundic glands. The parietal cells secrete hydrochloric acid and internal factors, the chief cells secrete pepsinogen, the enterochromaffin-like (ECL) cells in endocrine cells secrete histamine, G cells secrete gastrin, D cells secrete gastrin, and cervical mucus cells secrete mucus. The organoids can last for more than a year without losing the ability to expand or differentiate¹⁵.

In addition, the three-dimensionally cultured gastric organoids have complex 3D structures with structures and functions similar to those of internal organs^{16,17}. The gastric organoids are mostly cystic, and some gradually grow a bud-like structure around the cyst. There is no difference in the culture time, the expansion ratio, the expression of the gene markers of each constituent cell, or the cell type in the gastric organoids derived from a single gastric stem cell and from the gastric gland¹⁵.

Organoids can also be cultured in two dimensions, and electron microscopic observation reveals that the apical membrane of the stomach of the two-dimensional culture is oriented toward the medium⁴. Since the gastric epithelium is a special polar epithelial cell, we found that the apical membrane of the gastric organoid faces the inner cavity by staining the apical membrane marker ezrin, and the polarity distribution is in consistency with the gastric mucosal epithelial cells.

The gastric organoids both replicate the complexity of the disease phenotype in vivo while retaining the accessibility of in vitro. Gastric organoids that can be cultured in vitro for a long time have enabled researchers to overcome many obstacles and conduct basal and translational studies^{18,19}. Because it is closer to the environment in vivo, it is more faithful to physiology and pathology. Although organoids have their own limitations, bioengineering methods such as time-dependent and spatial-temporal materials can control the growth of organoids toward the desired structural form and self-organization, and other studies are already available. Vascular networks are added to organoid cultures to increase nutrients in a nearly physiological way^{20,21}. Co-culture methods for organoids can also mimic multiple organ lesions²².

In this study, after different concentrations of EtOH were added to murine gastric organoids for 1 hour, and after trypan blue staining, murine gastric organoids showed different degrees of positive trypan blue staining, indicating the impairment caused by EtOH. The extent of the damage of the gastric organoids depended on the concentration. Ethanol increases the permeability of parietal cell membranes²³ and triggers an increase in Ca^{2+} . Ethanol and endogenous aldehydes impaired chromosomal and variant stem cells²⁴.

Clinically, a variety of diseases and gastric acid secretion abnormalities are related, including gastroesophageal reflux disease, chronic gastritis, gastric ulcer, benign and malignant tumors of the gastrointestinal tract, anemia and so on.

In vivo methods for detecting gastric acid secretion in animal models often require an invasive procedure after anesthesia is fixed in the animal, and the secreted gastric acid is collected after catheterization into the stomach and is subsequently measured²⁵. The in vitro gastric acid detection method is more commonly used in the ¹⁴C aminopyrine experiment which was first proposed by Berglindh and Obrink in 1976²⁶. Due to the investigator's radioisotope experimental qualifications, the ¹⁴C aminopyrine test was temporarily unable to detect gastric acid.

Despite this, we observed that the number and location of most H^+ , K^+ -ATPase were not significantly changed in experiments of western blotting and immunofluorescence, but in repeated experiments, we observed H^+ , K^+ -ATPase is activated in the control group and diffused in the alcohol group (data not shown), suggesting that alcohol inhibition of gastric acid secretion may be related to the activation of H^+ , K^+ -ATPase, possibly due to its short spontaneous activation time. A statistically significant number of activated H^+ , K^+ -ATPases are to be further explored in future experiments using H^+ , K^+ -ATPase lentivirus-infected organoids.

From the results, we found that ethanol mediated the hydrolysis of ezrin, which was indicated by a specific hydrolysis zone at 55kD. After being impaired by 6% EtOH with different time intervals, a similar trend also emerged. The wrapping of Matrigel may have a certain physical protection effect on gastric organoids.

In this study, two methods were used to establish the ethanol-impairment models. The first one was to add ethanol to the medium to simulate the effect of alcohol concentration in the blood on murine gastric organoids. The advantage of this method was that it was more feasible. The disadvantage was that when the ethanol concentration is greater than or equal to 10%, the Matrigel collapsed.

In the view of the fact that the gastric organoids are similar to the stomach and are hollow cystic structures of the lumen, we have explored the use of microinjection techniques to directly inject ethanol into the internal gastric organoids to simulate gastric gavage. It was found that this modeling method could avoid the influence of Matrigel on the drug, and can be used to study the direct interaction of alcohol or pathogen-host, and at the same time, due to the surface tension of murine gastric organoids and the tight connection between cells, when the concentration of EtOH reached up to 50%, the Matrigel remained intact. When 6% alcohol was injected into the cavity, no obvious impairment was observed, and it may be related to the dilution of the ethanol concentration with a small amount of liquid in the cavity. Because the intracavitary volume of the stomach was temporarily unable to be accurately estimated, it was difficult to determine the specific final concentration of ethanol injected into the cavity. In addition, it took a certain time to microinject each organoids, and it is inconvenient to carry out protein immunization after drug stimulation. So, we chose the first modeling method that was more suitable for our experimental purposes.

BAPTA-AM [1,2-bis(2-aminophenoxy)ethane-N,N,N',N'-tetraacetic acid] is a cell permeable chelating agent with high selectivity for Mg^{2+} and Ca^{2+} , which can be used to control intracellular Ca^{2+} levels and chelate intracellular calcium ions. BAPTA has a higher selectivity for Ca^{2+} than EDTA[Ethylene glycol bis(2-aminoethyl Ether)-N,N,N',N'-tetraacetic acid] and EGTA, and its metal binding is also less sensitive to change of pH result. In this experiment, BAPTA chelated intracellular calcium ions, and the decrease of intracellular calcium ions caused the hydrolysis of ezrin to be significantly reduced compared with the alcohol group. EGTA chelated extracellular calcium ions, which reduced the influx of calcium ions, and decreased the intracellular calcium ion, so hydrolysis of ezrin was significantly reduced compared with the alcohol group.

E64d (molecular formula C₁₇H₃₀N₂O₅, relative molecular mass 342.4) is a specific calcium-activated neutral cysteine-based endopeptidase inhibitor with good cell membrane permeability and high selectivity for cysteine proteases. It can form a covalent bond with the cysteine thiol group at the active site of calpain, inhibiting its hydrolysis ability, and has a protective effect on alcohol-mediated gastric mucosal epithelial damage. In the E64d group, the hydrolysis of ezrin was significantly reduced, indicating that inhibition of calpain I activity was a factor determining the hydrolysis of ezrin, and demonstrated the role of calpain I-ezrin interaction in the mechanism of alcohol-mediated impairment of gastric organoids.

Calpain digests ezrin on parietal cells and impaired gastric acid secretion^{23,27}. Ezrin in parietal cells binds to the apical membrane during resting and stimulating phases^{28,29}, while some studies have suggested that ezrin was released from the apical membrane into the cytosol at rest in parietal cells³⁰.

Conclusion

In summary, hydrolysis of gastric ezrin reflects Ca²⁺-dependent protease activity. The in-situ hydrolysis of ezrin was blocked by the transmembrane cytoplasmic protease inhibitor E64d, which enhanced the important role of calpain I in the hydrolysis of parietal cells Ezrin. Our results indicated that calpain I was present in gastric parietal cells and that ezrin was a substrate within the cell of calpain I, and the impairment by EtOH was demonstrated by protein immunoblotting from the level of the human organoids as well, which indicated that this mechanism may also applicable in human.

Methods

Ethics Statement

Mouse experiments were performed in accordance with the Guide for the Care and Use of Laboratory Animals of the National Institutes of Health and following the International Guiding Principles for Biomedical Research Involving Animals. Protocols were approved by the Institutional Animal Care and Use Committee of Beijing University of Chinese Medicine.

Source of animals

All animals (C57BL/6 mouse) were obtained from Vital River Laboratory Animal Technology C.,Ltd. Animal production license No.: SCXK (Beijing) 2016-0006

Establishment of gastric organoids

For murine gastric organoids, SPF C57BL / 6 mice of 6-8 weeks were euthanized with CO₂, and then the stomach was dissected out and washed in cold DPBS (Sigma-Aldrich, D8537), inverted, tied and injected with DPBS to inflate, and then the stomach was put into a 15 ml tube of 5 ml DPBS containing 5 mM EDTA and placed on a 4 °C-degree shaker and slowly shaken for 2-2.5 hours. After that, 5mL shaking buffer was added, and the stomach was shaken in a 15ml tube by hand for about 3 minutes with an

interval of more than 1 second. At the end of 3 minutes, 20 μ l suspensions were taken to observe the gastric glands under the microscope. Generally, 20 μ l suspension usually contained about 20-50 gastric glands. Two 15 ml tubes containing 5 ml gastric glands were centrifuged at 4 °C and 300 g for 5 minutes. Appropriate amount of Matrix(BD Bioscience, 354263) containing the following growth factors were mixed with the glands: 50ng/ml EGF(Invitrogen, PHG 0313) 100ng/ml murine-noggin(Peprtech,250-38) 500ng/ml murine R-spondin (Peprtech, 315-32) 10nM Gastrin (Tocris,3006) 100ng/ml FGF10(Thermo Fisher,PMG0035) 100ng/ml mouse Wnt3A (Peprtech, 315-32) 2 μ mol/L TGF- β inhibitor(TOCRIS,2939) and 10 μ M RHOK-inhibitor(Tocris,1254) .The 8-well chamber (Thermo Scientific, 155411) was put in the incubator at 37°C for 30 minutes to allow Matrigel to polymerize fully, and culture media was added to the 8-well chamber. Cultures were kept at 37°C in a 5% CO₂ incubator and the medium were refreshed every 2-3 days. Organoids were passaged every 6-7 days at a ratio of about 1:4. Statistical significance was defined as $p < 0.05$. All statistical analyses were calculated using GraphPad Prism (Version 5.2). All experiments were performed with at least 3 biological replicates ($n \geq 3$), each analyzed in at least 2 technical replicates.

For human gastric organoids, the detailed protocol was as documented before¹⁵. In short, the gastric tissues of patients were placed in basic medium, and the mucus and muscular layers were carefully removed, and then the tissues were cut into 20-50 small pieces. After being washed by shaking buffer, the gastric glands were extracted and embedded in Matrigel (BD Biosciences,354263), and overlaid with advanced Dulbecco's modified Eagle medium (DMEM/F12) (Gibico, 12634010) containing penicillin/streptomycin (Invitrogen, 15140122), 10 mM HEPES(Invitrogen, 15630080), GlutaMAX (Invitrogen, 35050061), 1 \times B27 (Invitrogen, 17504-044) and the following growth factors: 50ng/ml EGF(Invitrogen, PHG0313), 100ng/ml human noggin (Peprtech, 120-10C), 500ng/ml human R-spondin (Peprtech, 315-32), 1nmol/L Gastrin (Tocris,3006), 200ng/ml hFGF10 (Peprtech,100-26), 50% Wnt-conditioned-medium, 2 μ mol/L TGF- β inhibitor A-83-01 (Tocris,2939), 10 μ mol/L rho-associated coiled coil forming protein serine/threonine kinase RHOK-inhibitor (Tocris,1254). In general, the passages of 2-5 of organoids from three different preparations were applied in our experiments without noticed difference in morphology. The study was approved by the Ethics Committee of the Dongzhimen Hospital of the Beijing University of Chinese Medicine.

Microinjection

The glass capillary with 1mm diameter was pulled into the required length and diameter by the program-controlled micropipette puller, and then the tip was cut by sharp blade and the end of the capillary was about 10 μ m. Next, the capillary was filled with ethanol solution by microloader tip (Eppendorf), and then the organoids were placed under the stereomicroscope, and each organoid was inhaled about 0.2 μ L suspension.

Trypan blue staining

For vital staining, gastric organoids were incubated with trypan blue for 2-5 minutes, washed 3 times with PBS, left in 37°C for another 15 minutes with PBS, washed again and visualized.

Immunofluorescence

Gastric organoids were fixed with 4% FA for 10 minutes. For the analysis, organoids were permeabilized with 0.2% Triton X-100 and blocked in 5% BSA for 30 minutes. Ezrin (1:200, abcam, ab235927), H⁺, K⁺-ATPase (abcam, ab2G11, 1:1000), were incubated with the organoids overnight at 4°C. Next, organoids were incubated with Alexa Fluor 488 or 633 (1:1000, Invitrogen) for 1 hour at room temperature, followed by nuclear stain (DAPI, Invitrogen) for 10 min. Whole mount sections were obtained via Z-stack reconstruction using confocal microscope (Zeiss LSM880).

Western blotting

Gastric organoids were cultured for 6 days and removed from Matrigel[®] BD Bioscience #356237 using Cell Dissociation Solution[®] Sigma-Aldrich C5914. Cell lysates were prepared in RIPA buffer (50 mM Tris-HCl, 150 mM NaCl, 1 mM EDTA, 1% NP-40, 0.5% deoxycholate, 0.1% sodium dodecyl sulfate) with protease inhibitors. After separation by SDS-PAGE, immunoblots were probed for Ezrin (abcam, ab235927, 1:1000) antibody, Anti-H⁺, K⁺-α-ATPase antibody (abcam, ab2G11, 1:1000), or GAPDH antibody (Sungene Biotech, 1:5000), and the second antibody were either HRP-conjugated anti-mouse antibody (Jackson Immuno Research) or HRP-conjugated anti-rabbit antibody (Jackson Immuno Research), and the membranes were visualized with chemiluminescence[®] Millipore-Sigma WBKLS0500.

Statistical analysis

The statistical analysis was performed using the statistical package for the social sciences (SPSS, version 13.0, Chicago, IL). The non-normally distributed data were expressed as the median (quartile range). The within group differences were assessed using a non-parametric test while the Wilcoxon rank test was used to compare two groups. The normally distributed data and homogeneous variances were expressed as the mean ± standard deviation (SD). Multiple comparisons were performed using a one-way analysis of variance (ANOVA) followed by the least significant difference (LSD) test. A *p* value <0.05 was considered statistically significant for the analyses.

Abbreviations

EtOH: ethyl alcohol

Declarations

Ethics approval and consent to participate

Ethics committee of Beijing University of Chinese Medicine (2018BZHYLL0103), Ethics committee of University of Science and Technology of China (USTCACUC1801024).

Consent for Publication

Not applicable.

Availability of data and material

All data generated or analyzed during this study are included in this published article.

Competing interests

The authors declare that they have no competing interests.

Funding

This work was supported by the National Natural Science Foundation of China (81630080). The funding body had no role in the design of the study and collection, analysis, and interpretation of data and in writing the manuscript.

Authors' contributions

The conception and design of the work: XL, XD. Acquisition of data: WJW, YZ, ZQS, FHC, TL, YL, XYS, XUL. Analysis and interpretation of data: all coauthors. Drafting of the manuscript: WJW, YZ, XL, and XD. Statistical analysis: WJW, YZ, XUL, XL, XD. All authors have read and approved the manuscript.

Acknowledgements

We thank Professor Fang Zhiyou for technical assistance and members of our groups in Beijing University of Chinese Medicine, University of Science and Technology of China, and 1st Hospital affiliated to Anhui Medical University.

References

1. Garaycochea J I, Crossan G P, Langevin F, et al. Alcohol and endogenous aldehydes damage chromosomes and mutate stem cells. *Nature*, 2018, 553(7687):171-177.
2. Hanzel DK, Urushidani T, Usinger WR, et al. Immunological localization of an 80-kDa phosphoprotein to the apical membrane of gastric parietal cells. *American Journal of Physiology*, 1989, 256: 1082-1089.
3. Urushidani T, Hanzel DK, Forte JG. Protein phosphorylation associated with stimulation of rabbit gastric glands. *BBA - Molecular Cell Research*, 1987, 930: 209-219.
4. Akisawa N, Nishimori I, Iwamura T, et al. High levels of Ezrin expressed by human pancreatic adenocarcinoma cell lines with high metastatic potential. *Biochemical & Biophysical Research Communications*, 1999, 258: 395-400.

5. Yao X, Forte JG. Cell biology of acid secretion by the parietal cell. *Annual Review of Physiology*,2003,65:103-131.
6. Tamura A, Kikuchi S, Hata M, et al. Achlorhydria by Ezrin knockdown: defects in the formation/expansion of apical canaliculi in gastric parietal cells. *Journal of Cell Biology*, 2005, 169: 21-28.
7. Saotome I, Curto M, McClatchey AI. Ezrin Is Essential for Epithelial Organization and Villus Morphogenesis in the Developing Intestine. *Developmental Cell*, 2004, 6: 855-864.
8. Clevers H. Modeling Development and Disease with Organoids. *Cell*, 2016, 165: 1586-1597.
9. Lancaster MA, Knoblich JA. Organogenesis in a dish: modeling development and disease using organoid technologies. *Science*, 2014, 345: 1247125.
10. Sina Bartfeld, Hans Clevers. Organoids as Model for Infectious Diseases: Culture of Human and Murine Stomach Organoids and Microinjection of Helicobacter Pylori. *Journal of Visualized Experiments*, 2015, 2015(105):816-818.
11. Pageot LP, Perreault N, Basora N, et al. Human cell models to study small intestinal functions: Recapitulation of the crypt-villus axis. *Microscopy Research and Technique*, 2000, 49: 394-406.
12. Young DF, Carlos TS, Hagmaier K, et al. AGS and other tissue culture cells can unknowingly be persistently infected with PIV5; A virus that blocks interferon signaling by degrading STAT1. *Virology*, 2007, 365: 238-240.
13. Tung YC, Hsiao AY, Allen SG, et al. High-throughput 3D spheroid culture and drug testing using a 384 hanging drop array. *Analyst*, 2011, 136: 473-478.
14. O'Rourke JL, Lee A. Animal models of Helicobacter pylori infection and disease. *Microbes & Infection*, 2003, 5: 741-748.
15. Sina B, Tülay B, Marc VDW, et al. In vitro expansion of human gastric epithelial stem cells and their responses to bacterial infection. *Gastroenterology*, 2015, 148: 126-136.e126.
16. Lancaster M A, Knoblich J A. Organogenesis in a dish: Modeling development and disease using organoid technologies. *Science*,2014, 345(6194):1247125-1247125.
17. Sina B, Tülay B, Marc VDW, et al. In vitro expansion of human gastric epithelial stem cells and their responses to bacterial infection. *Gastroenterology*, 2015, 148: 126-136.e126.
18. Bartfeld S, Clevers H. Organoids as Model for Infectious Diseases: Culture of Human and Murine Stomach Organoids and Microinjection of Helicobacter Pylori. *Journal of Visualized Experiments*,2015,43:816-818.
19. Barker N, Huch M, Kujala P, et al. Lgr5+ve Stem Cells Drive Self-Renewal in the Stomach and Build Long-Lived Gastric Units In Vitro. *Cell Stem Cell*, 2010, 6: 25-36.
20. Yui S, Nakamura T, Sato T, et al. Functional engraftment of colon epithelium expanded in vitro from a single adult Lgr5⁺ stem cell. *Nature Medicine*, 2012, 18: 618-623.
21. Miller JS, Stevens KR, Yang MT, et al. Rapid casting of patterned vascular networks for perfusable engineered three-dimensional tissues. *Nature Materials*,2012,11:768-774.

22. Wang XY, Jin ZH, Gan BW, et al. Engineering interconnected 3D vascular networks in hydrogels using molded sodium alginate lattice as the sacrificial template. *Lab on a Chip*, 2014, 14: 2709-2716.
23. Workman MJ, Mahe MM, Trisno S, et al. Engineered human pluripotent-stem-cell-derived intestinal tissues with a functional enteric nervous system. *Nature Medicine*, 2017, 23: 49-59.
24. Yao X, Thibodeau A, Forte JG. Ezrin-calpain I interactions in gastric parietal cells. *American Journal of Physiology*, 1993, 265: 36-46.
25. Garaycochea JI, GP C, F L, et al. Alcohol and endogenous aldehydes damage chromosomes and mutate stem cells. *Nature*, 2018, 553: 171-177.
26. Xia ZF, Fritze DM, Li JY, et al. Nesfatin-1 inhibits gastric acid secretion via a central vagal mechanism in rats. *Am J Physiol Gastrointest Liver Physiol*, 2012, 303: G570.
27. Obrink TBHFHKJ. Effects of Secretagogues on Oxygen Consumption, Aminopyrine Accumulation and Morphology in Isolated Gastric Glands. *Acta Physiologica Scandinavica*, 1976, 97: 401-414.
28. Wang H, Guo Z, Wu F, et al. PKA-mediated protein phosphorylation protects Ezrin from calpain I cleavage. *Biochemical & Biophysical Research Communications*, 2005, 333: 496-501.
29. Zhu L, Hatakeyama J, Chen C, et al. Comparative study of Ezrin phosphorylation among different tissues: more is good; too much is bad. *Am J Physiol Cell Physiol*, 2008, 295: C192.
30. Lahavbaratz S, Sudakin V, Ruderman JV, et al. Reversible phosphorylation controls the activity of cyclosome-associated cyclin-ubiquitin ligase. *Proceedings of the National Academy of Sciences of the United States of America*, 1995, 92: 9303-9307.
31. Sawaguchi A, Aoyama F, Ohashi M, et al. Ultrastructural transformation of gastric parietal cells reverting from the active to the resting state of acid secretion revealed in isolated rat gastric mucosa model processed by high-pressure freezing. *Journal of Electron Microscopy*, 2006, 55: 97.

Figures

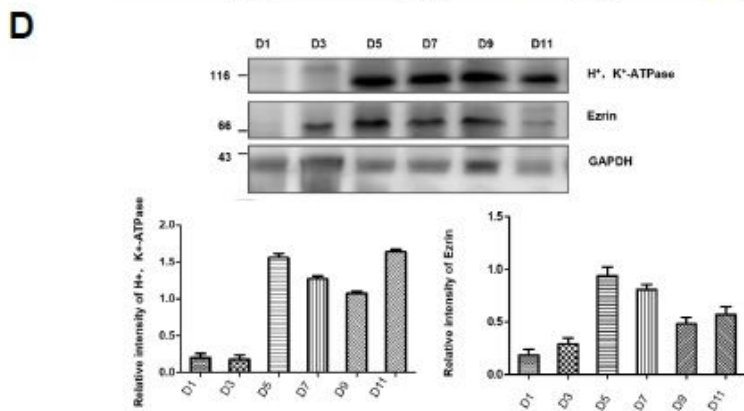
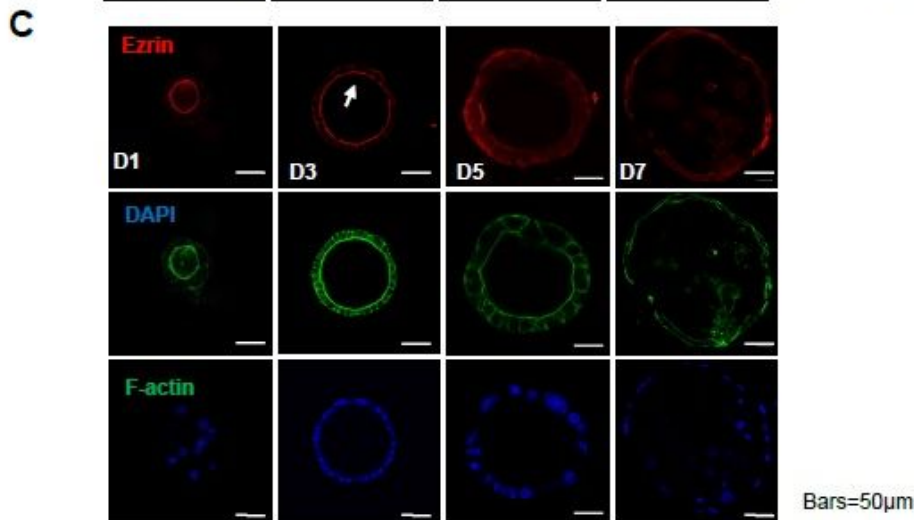
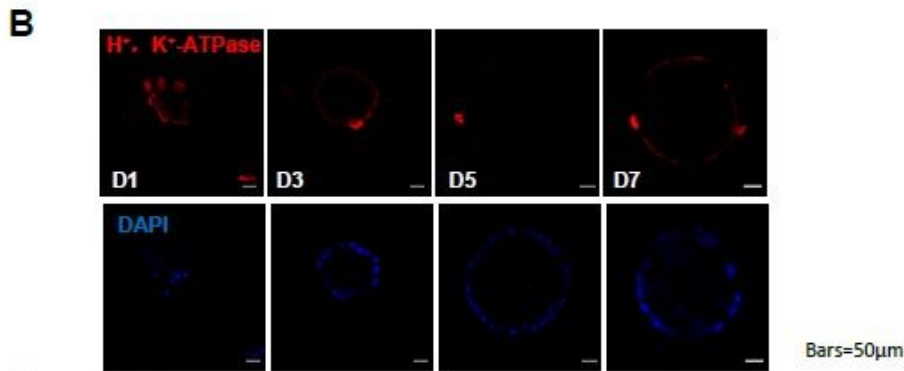
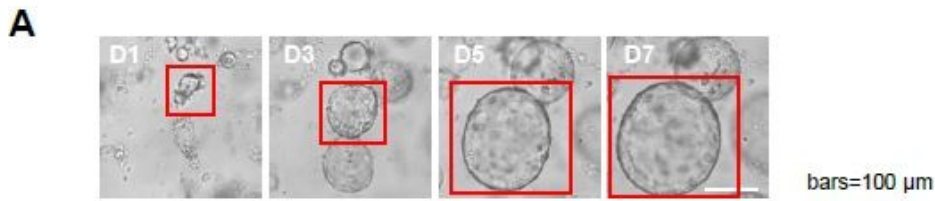


Figure 1

Establishment of murine gastric organoids. a DIC images of murine gastric organoids in Day 1 Day 3 Day 5 and Day 7 (Scale bars, 100 μm). b Immunofluorescent images of H⁺, K⁺ -ATPase in Day 1 Day 3 Day 5 and Day 7 (Scale bars, 50 μm). c Immunofluorescent images of ezrin in Day 1 Day 3 Day 5 and Day 7 (Scale bars, 50 μm). d Western blotting results of the changes of protein markers in murine gastric organoids.

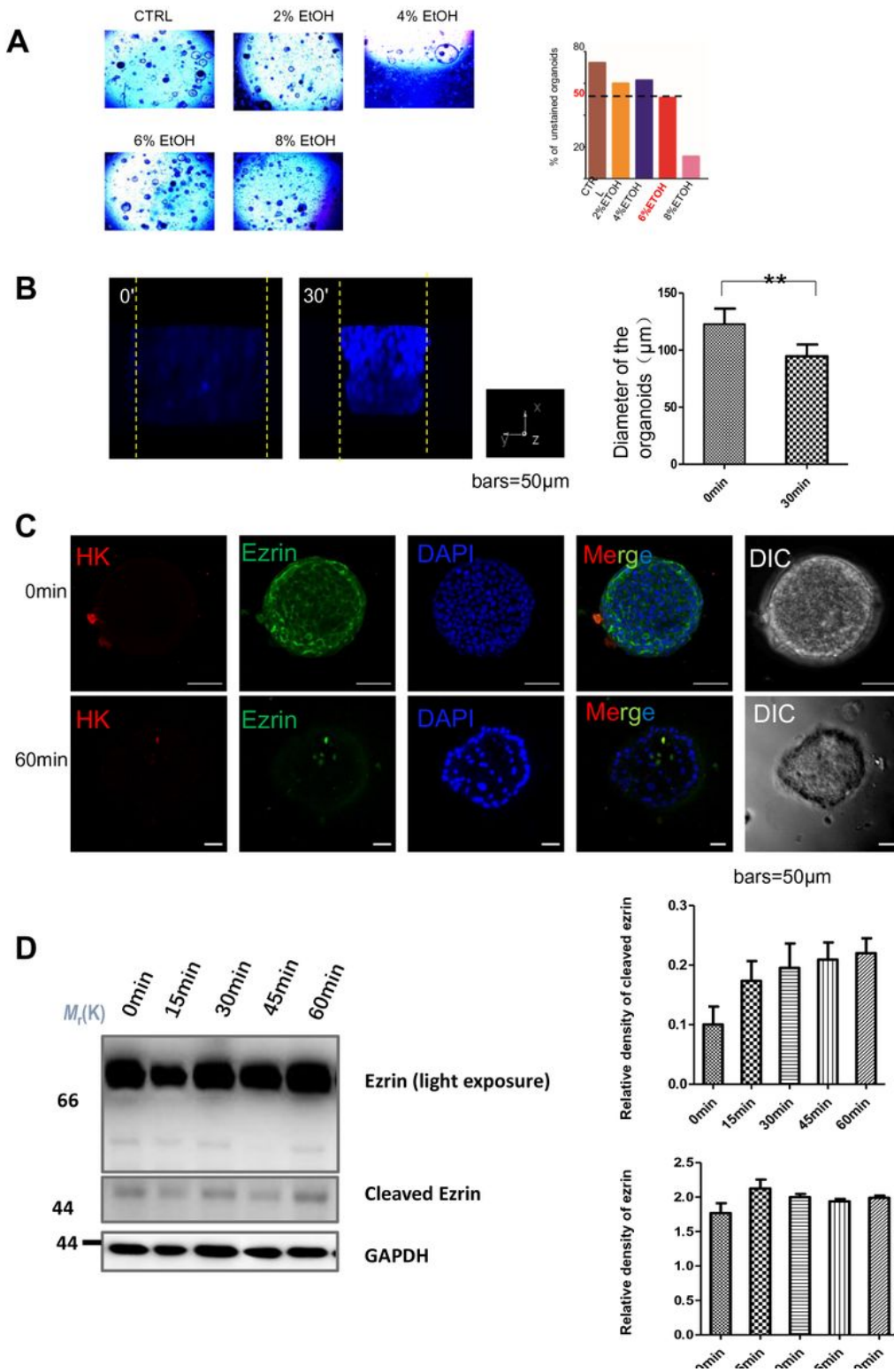


Figure 2

Ethanol impaired gastric organoids. a Trypan blue staining results of gastric organoids injured by EtOH with different concentrations (Bars= 200 µm). b Statistics of live cell photographs of gastric organoids impaired by EtOH. ** $p < 0.01$. c Immunofluorescent images of gastric organoids at 0 min and 60 min after being injured by 50% EtOH by microinjection. d Western blot results of 6% EtOH-induced impairment to murine gastric organoids. ** $p < 0.01$.

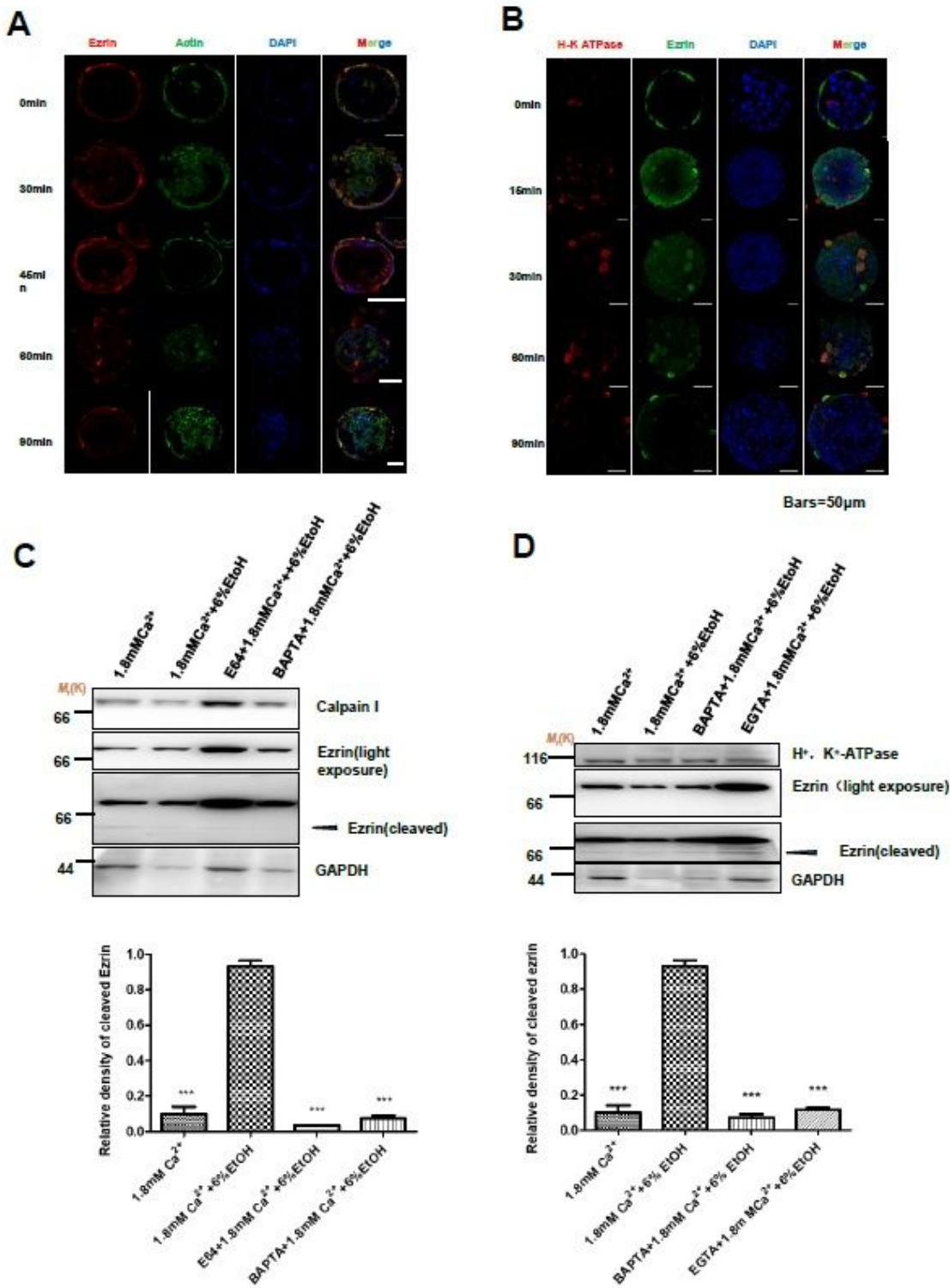


Figure 3

Ethanol-induced gastric organoids impairment was caused by calcium-dependent calpain activation. a Immunofluorescence of ezrin and F-actin in murine gastric organoids impaired by time gradient of 6% ethanol (bars= 50 μ m). b Immunofluorescence of ezrin and H⁺, K⁺-ATPase in murine gastric organoids with 6% ethanol by time gradient (bars = 50 μ m). c Western blotting and statistical analysis of murine gastric organoids of CaCl₂ group, 6% ethanol group, E64 group and BAPTA group. d Western blotting and

statistical analysis of murine gastric organoids of CaCl₂ group, 6% ethanol group, EGTA group and BAPTA group. ***p<0.001.

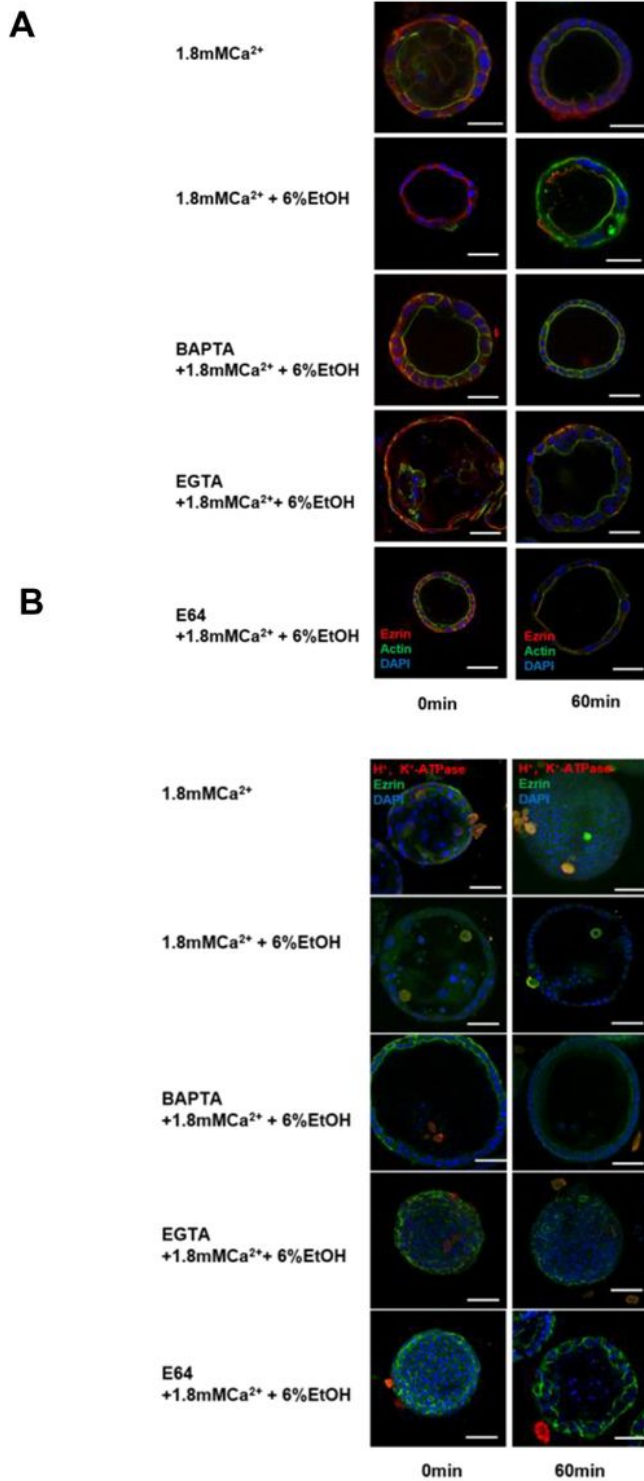


Figure 4

Ethanol-mediated calcium ion impairment on the localization of ezrin, H⁺, K⁺-ATPase and F-actin in murine organoids. a Immunofluorescence staining of ezrin, actin and DAPI in murine gastric organoids with ethanol-mediated calcium ion impairment (bars = 50 μm). b Immunofluorescence staining of ezrin,

H⁺, K⁺-ATPase and DAPI in murine gastric organoids with ethanol-mediated calcium ion impairment (bars = 50 μm).

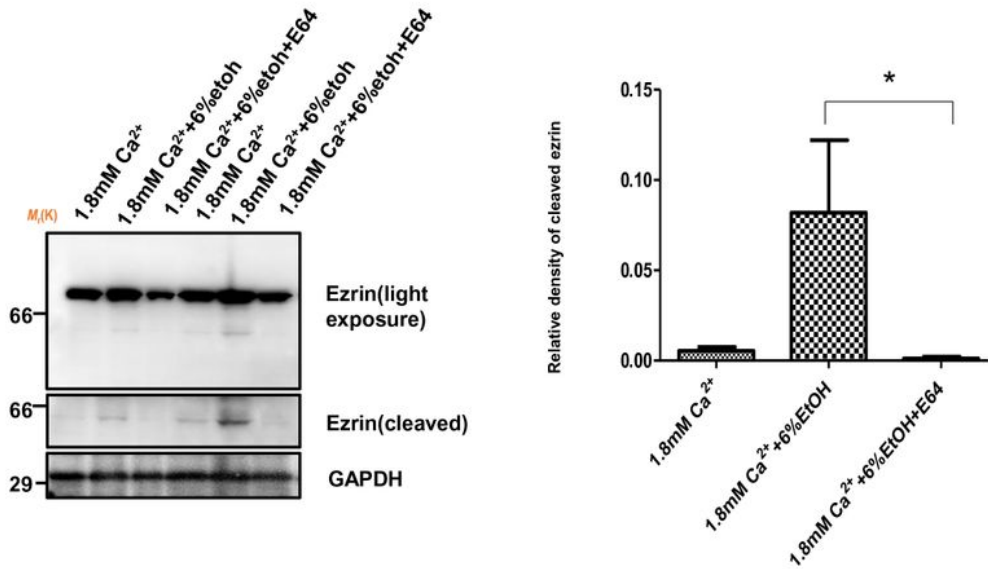


Figure 5

Western blot results of ethanol-mediated calcium ion impairment in human gastric organoids. Human gastric organoids were impaired either with 1.8 mM CaCl₂, 1.8 mM CaCl₂ plus 6% EtOH, or with 1.8 mM

CaCl₂ plus 6% EtOH plus E64, respectively. After 1 hour, the expressions of ezrin and actin were detected by western blot, and the values of the bands were measured with Image J. * p<0.05

Supplementary Files

This is a list of supplementary files associated with this preprint. Click to download.

- [additionalfile1uncroppedfigures.docx](#)
- [additionalfiles.docx](#)